Boletim da Sociedade Astronômica Brasileira, **36**, no. 1, 5-8

Pathways towards compact dwarf galaxies: Insights from TNG50

Abhner P. de Almeida[1,2], Gary A. Mamon[2], & Gastão B. Lima Neto[1]

[1] Instituto de Astronomia, Geofísica e Ciências Atmosféricas, USP, São Paulo, Brasil
[2] Institut d'Astrophysique de Paris (UMR 7095: CNRS & Sorbonne Université), 98 bis Bd Arago, F-75014 Paris, France
* abhner.almeida@usp.br

Abstract. Nearby dwarf galaxies display a variety of effective radii (size) at a given stellar mass, from dwarf spheroidals to compact ellipticals, suggesting diverse evolutionary mechanisms shaping that final stellar size. Using the TNG50 cosmological simulation, we explore the evolution of the most massive progenitors of dwarf galaxies to understand what drives the corpulence (size at a given stellar mass) of these galaxies. We classify the galaxies based on the z=0 mass-size relation: "Normals" follow the main mass-size relation; while "Compacts" have smaller sizes. Additionally, we separate our sample into centrals and satellite galaxies. At earlier times (z>2), all populations exhibit similar sizes. However, Central Compacts experience a decrease in size from z∼1. This compaction is driven by concentrated star formation fueled by the accretion of low-angular-momentum gas, which leads to an efficient gas infall. Satellite Compacts present two different mechanisms driving their size decrease, depending on the degree of the environmental interaction: those that have less influence evolve like the central counterparts; while the others depend on tidal stripping to become compact due the loss of stellar mass. Our conclusions highlight the complex interplay of internal and external mechanisms in shaping compact dwarf galaxies.

Resumo. Galáxias anãs no universo local exibem uma variedade de raios efetivos (tamanho) para uma dada massa estelar, de esferoidais anãs a elípticas compactas, sugerindo diversos mecanismos evolutivos que moldam o tamanho estelar final. Usando a simulação cosmológica TNG50, exploramos a evolução dos progenitores mais massivos de galáxias anãs para entender o que impacta na evolução da corpulência (tamanho em uma dada massa estelar) dessas galáxias. Classificamos as galáxias com base na relação massa-tamanho em z=0: "Normais" seguem a relação massa-tamanho principal; enquanto "Compactas" têm tamanhos menores. Além disso, separamos nossa amostra em galáxias centrais e satélites. Em alto redshift (z>2), todas as populações exibem tamanhos semelhantes. No entanto, as Compactas Centrais experimentam uma diminuição no tamanho a partir de z∼1. Essa compactação é impulsionada pela formação estelar concentrada alimentada pela acreção de gás de baixo momento angular, o que leva a um eficiente *infall* do gás. Compactas satélites apresentam dois mecanismos diferentes que impulsionam sua diminuição de tamanho, dependendo do grau de interação com o ambiente: aqueles que têm menos influência evoluem como as contrapartes centrais; enquanto a população restante depende dos efeitos de maré para se tornar compacta pela perda de massa estelar. Nossas conclusões destacam a interação complexa de mecanismos internos e externos na formação de galáxias anãs compactas.

Keywords. Galaxies: dwarf – Galaxies: evolution – Galaxies: interactions

1. Introduction

Dwarf galaxies are important laboratories for studying several physical mechanisms that govern galaxy formation and evolution (Haynes 2019). These mechanisms are present in the galaxy evolution and can be both internal and external to the galaxy. For internal mechanisms, supernova feedback (Dekel & Silk 1986) and central black hole activity (Silk & Rees 1998) have an important role. On the other hand, important external mechanisms are tidal interactions (Merritt 1983), ram-pressure stripping (Gunn & Gott 1983), and gravitational harassment (Moore et al 1996). These external forces are more important for satellite galaxies.

A key observable to studying stellar systems is the size–mass relation (SMR), which relates the galaxy's effective radius to its stellar mass. Dwarf galaxies (10^7–$10^9 M_\odot$) exhibit a bimodal size distribution in the SMR, presenting both diffuse (e.g., dwarf ellipticals) and compact (e.g., compact ellipticals and ultra-compact dwarfs) populations. Compact galaxies are often associated with dense environments, suggesting formation scenarios driven by tidal stripping of more massive progenitors (e.g Chilingarian & Mamon 2008; Brodie et al. 2011). However, their presence in isolated regions indicates alternative formation mechanisms, such as mergers (e.g. Bekki 2008) or the evolutionary result of extremely massive stellar clusters (e.g. Mieske et al. 2002).

Both *N*-body and hydrodynamic simulations can provide important insights to understand how the different mechanisms work to shape the galaxy during its evolution. For example, several works used tailored simulations (e.g. Bekki et al. 2001; Pfeffer & Baumgardt 2013), as well as large-scale cosmological simulations (e.g. Pfeffer et al. 2014), to study how tidal stripping can be important for the formation of compact dwarf galaxies.

Since cosmological simulations can provide valuable information about galaxy evolution in a more complex context, we use the data from the state-of-the-art cosmological simulation Illustris TNG50-1 (hereafter, TNG50) simulation (Nelson et al. 2019; Pillepich et al.), which is the best-resolved run in the IllustrisTNG (hereafter, TNG) suite of simulations (Springel et al. 2018; Pillepich et al. 2018; Marinacci et al. 2018; Naiman et al. 2018; Nelson et al. 2018), to understand what drives the corpulence of compact dwarf galaxies, both centrals and satellites. In this work, we present some results from our previous works de Almeida et al. 2024, hereafter **Paper I**, and de Almeida et al. 2024b, hereafter **Paper II**.

2. Methodology

Figure 1 shows the mass-size relation at $z = 0$ for TNG50, highlighting the objects we study in this work. We select galaxies with a stellar mass between $10^{8.4}$ and $10^{9.2}$ $M_\odot$, to guarantee

the best-resolved galaxies in the dwarf regime. We classify these galaxies into three different populations. We first select a control sample, refer to as Normals, which follow the main trend of the $z = 0$ mass-size relation. After that, we select two compact populations: Compacts$_{\rm MB}$, representing galaxies along the lower envelope of the main trend, and Compacts$_{\rm SB}$, consisting of galaxies with stellar half-mass radii ($r_{1/2,*}$) smaller than $\sim$ 450 pc. Furthermore, we split between galaxies that at the end of the simulation remain as centrals of their own halo and those that evolve into satellites of bigger halos.

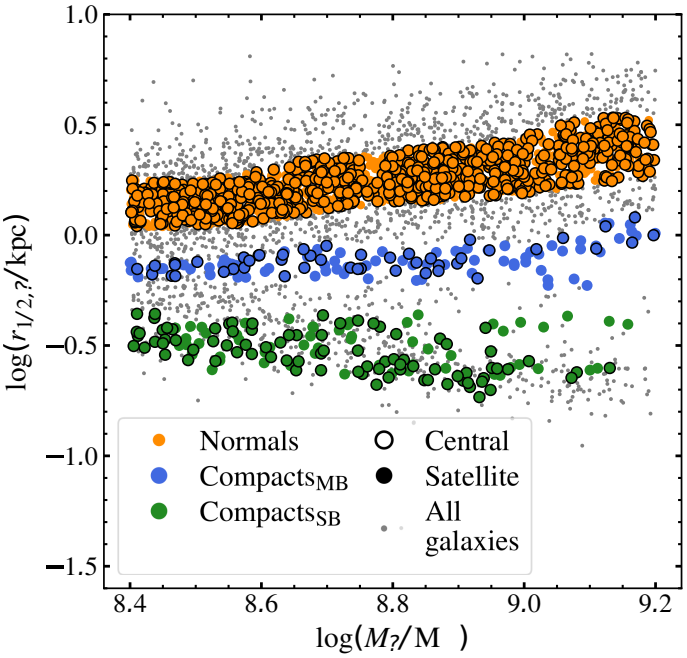

Figure 1. $z = 0$ stellar half-mass radius vs. stellar mass. The *orange*, *blue*, and *green circles* are the different populations, respectively: Normals, Compacts$_{\rm MB}$ (Main branch) and Compacts$_{\rm SB}$ (Secondary branch). Those circles with (without) *black edge lines* are for centrals (satellites). The *gray dots* are all the subhalos in the stellar mass range.

Since satellite galaxies are selected based on their status at the end of the simulation, we can have both satellite galaxies that become satellite just before the end of the simulation and galaxies that become satellite earlier in the simulation. In these different cases the impact of the environment will be different. To account for this, we compare two parameters for each satellite galaxy: the final dark matter (DM) mass normalized by the maximum DM mass in the galaxy evolution and the final DM fraction. The normalized DM mass is a direct proxy to tidal stripping, reflecting the loss of DM mass due to environmental effects, while DM fraction is a somewhat observable parameter. Figure 2 demonstrates a strong correlation between the final DM fraction and the normalized DM mass. We therefore adopt the final DM fraction as our proxy for environment interaction. Therefore, we end-up with DM-rich and DM-poor satellite galaxies according to whether the $z = 0$ DM fraction is above or below 0.7. DM-rich satellites, with higher final DM-fractions, have experienced less DM mass loss and are thus less influenced by their environment compared to DM-poor satellites.

After the selection, we analyze the median evolution of different galaxy properties in order to identify the mechanisms driving the compaction of dwarf galaxies. For each population, we compute the median value of specific parameters at each snapshot within the simulation. We estimate the median uncertainties using bootstrap. Also, we compute median radial profiles of some parameters for some snapshots. Further details are provide in **Paper I** and **Paper II**.

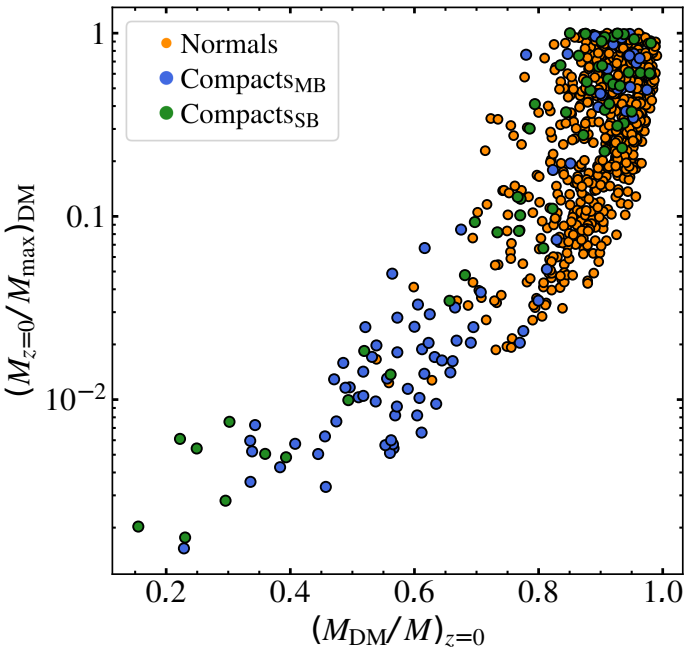

Figure 2. $z = 0$ DM fraction vs. final DM mass normalized by the maximum DM mass in the galaxy evolution. The colors indicate the same as Fig. 1.

3. Results

Figure 3 shows the evolution of half-mass radius and specific stellar formation rate (sSFR) within the half-mass radius (hereafter inner sSFR) for the different populations. At earlier times ($z > 1$ for centrals and DM-rich satellites, and $z > 1.5$ for DM-poor satellites), all Compact populations present similar size compare to Normals. After $z \sim 1$, central Compacts start to decrease in size, which is more pronounced for the Compacts$_{\rm SB}$. Similarly, DM-rich satellites also experience a size decrease after $z \sim 1$, although they already show slightly smaller size compared to Normals. Meanwhile, DM-poor Satellite Compacts begin to diverge from their Normal counterparts at $z \sim 2$, as the Normals continuous to grow in size while these Compacts maintain a constant size until $z \sim 1$, after which they also begin to decrease in size.

Regarding the inner sSFR, Fig. 3 shows that Central and DM-rich Satellite Compacts have very similar trends, while DM-poor Satellite Compacts experience quenching at $z \sim 0.6$ and $z \sim 0.2$ for Compacts$_{\rm MB}$ and Compacts$_{\rm SB}$, respectively. This quenching is likely driven by ram-pressure, as expected since we select DM-poor as those that have more influence from the interaction with the environment. Besides to keep their star formation until the end of the simulation, Centrals and DM-rich Satellites are able to maintain their inner sSFR almost constant and higher than the Normals after $z \sim 1$, whereas this latter population show a continuous decrease of inner sSFR. These suggest that star formation can play a significant role in driving compaction for Centrals and DM-rich Satellites. This is further supported by the fact that those Compacts that end with smaller sizes, Compacts$_{\rm SB}$, have higher inner sSFR compared to Compacts$_{\rm MB}$.

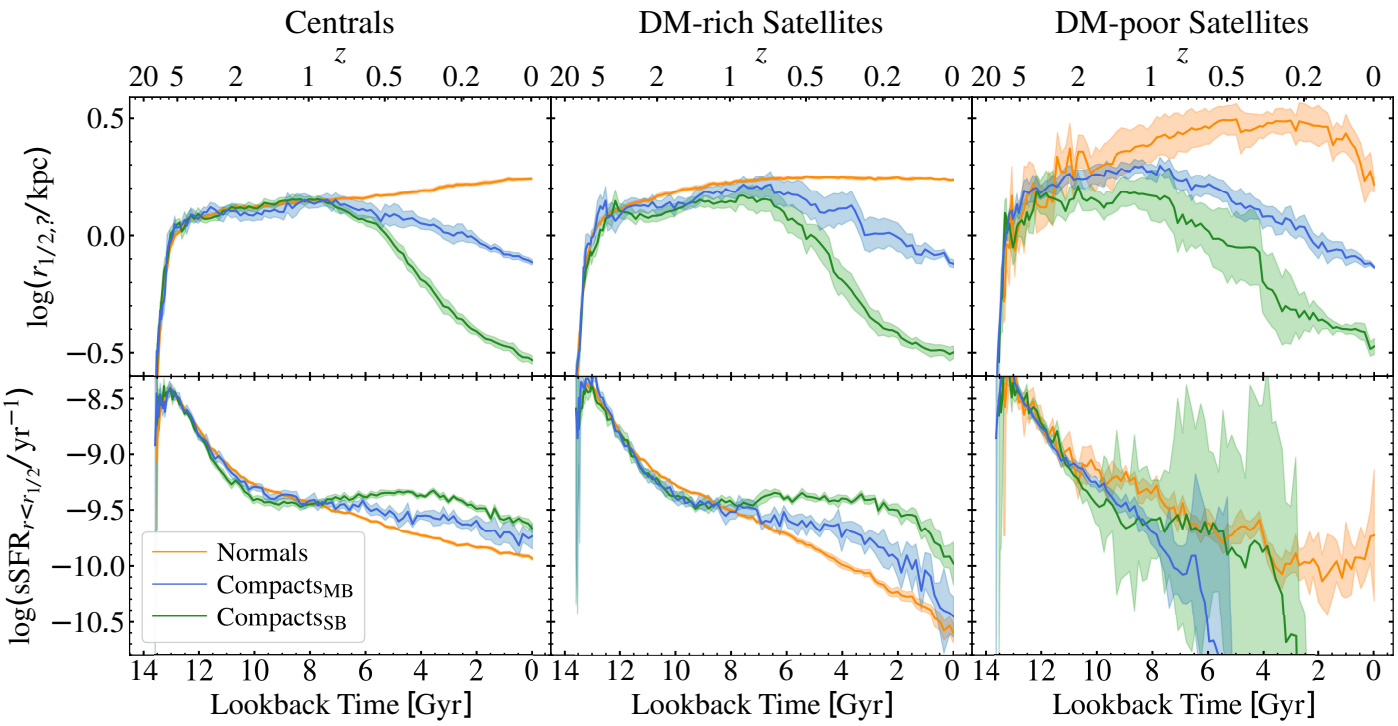

Figure 3. Half-mass radius (**top**) and inner sSFR (**bottom**) evolution. The **left**, **middle** and **right** columns are for centrals, DM-rich satellites, and DM-poor satellites, respectively. The colors indicate the same as Fig. 1.

To better understand the role of inner star formation in compaction, we compare the stellar density profiles at different snapshots. While the inner star formation doesn't seem to be important for the evolution of DM-poor Satellites, as they quench before the end of the simulation, the lose of outer stellar material due tidal stripping may have an impact. Analyzing the stellar density profile can also provide valuable insights into this process.

Figure 4 shows the stellar density profiles at the end of the simulation, and at an earlier snapshot: at $z_{\rm earlier} = 1$ (for centrals and DM-rich Satellites), and at $z_{\rm earlier} = z_{\rm entry}$ (for DM-poor Satellites). The $z_{\rm entry}$ corresponds to the moment when a satellite galaxy first crosses the R_{200} of its host group. Central and DM-rich Satellite experience a large increase of inner stellar content compared to their Normal counterparts between $z_{\rm earlier} = 1$ to $z = 0$. This growth is consistent with the fact that compact galaxies are able to maintain their inner star formation higher than Normals as seen in Fig. 3. In contrast, DM-poor galaxies likely to lose a substantial amount of their outer stellar content between $z_{\rm earlier} = z_{\rm entry}$ to $z = 0$, likely due to tidal stripping. Interestingly, DM-poor satellite Compacts$_{\rm SB}$ present a significant increase in inner stellar content after $z$entry, suggesting that,for these galaxies, inner star formation may also play an important role alongside tidal stripping.

4. Conclusions

In the present work, we aim to understand what drives the corpulence of compact dwarf galaxies using data from the TNG50 cosmological hydrodynamical simulation. Our analysis focuses on both central and satellite dwarf galaxies with stellar log masses between 8.4 and 9.2 $M_\odot$, divided into three populations based on the $z = 0$ mass–size relation: Normals, which follow the main size–mass trend; Compacts$_{\rm MB}$, representing the lower envelope of the main branch; and Compacts$_{\rm SB}$, characterized by half-stellar-mass radius lower than 0.45 kpc. For satellite galaxies, we further classify them by their final DM fraction: DM-poor Satellites, are those that lose more DM material, which is related to an important impact from environment interactions; while DM-rich Satellites lose less DM material, corresponding to those that have less influence by environment. Due the lower influence by environment, DM-rich Satellite have a similar evolution compare to Central galaxies.

For Central and DM-rich Satellite Compacts, compaction occurs after $z \sim 1$ as they are able to maintain higher inner star formation compared to the Normal galaxies. This concentrated inner star formation leads to a large increase of stellar content in the inner region, which in turn leads the galaxy to become more compact. As detailed in **Paper I**, the higher inner star formation of Central Compacts is related to the accretion of low-angular-momentum gas, which efficiently funnels into the inner region of the galaxy, sustaining the reservoir for star formation. This same mechanism also occurs in DM-rich satellite Compacts, as explored in more details in **Paper II**.

In contrast, DM-poor satellite Compacts become compact by losing outer stellar material through tidal stripping. In the previous moments before the quenching, these galaxies also can count on inner star formation to become compact. In **Paper II** we discussed in more details the interplay between inner star formation and tidal stripping, showing that since ram-pressure act first to remove outer gas material, the galaxy is able to maintain its inner star formation until the total quenching. This helps the compaction, although the tidal stripping is the main mechanism to drive the compaction.

Our analysis reveal two main pathways for dwarf galaxy compaction: (1) concentrated star formation, typical of Centrals and DM-rich Satellites, and (2) tidal stripping, dominant in DM-poor Satellites. Future spectroscopic studies of Compact dwarfs, combined with high-resolution hydrodynamic simulations, can verify and refine our results on dwarf galaxy evolution.

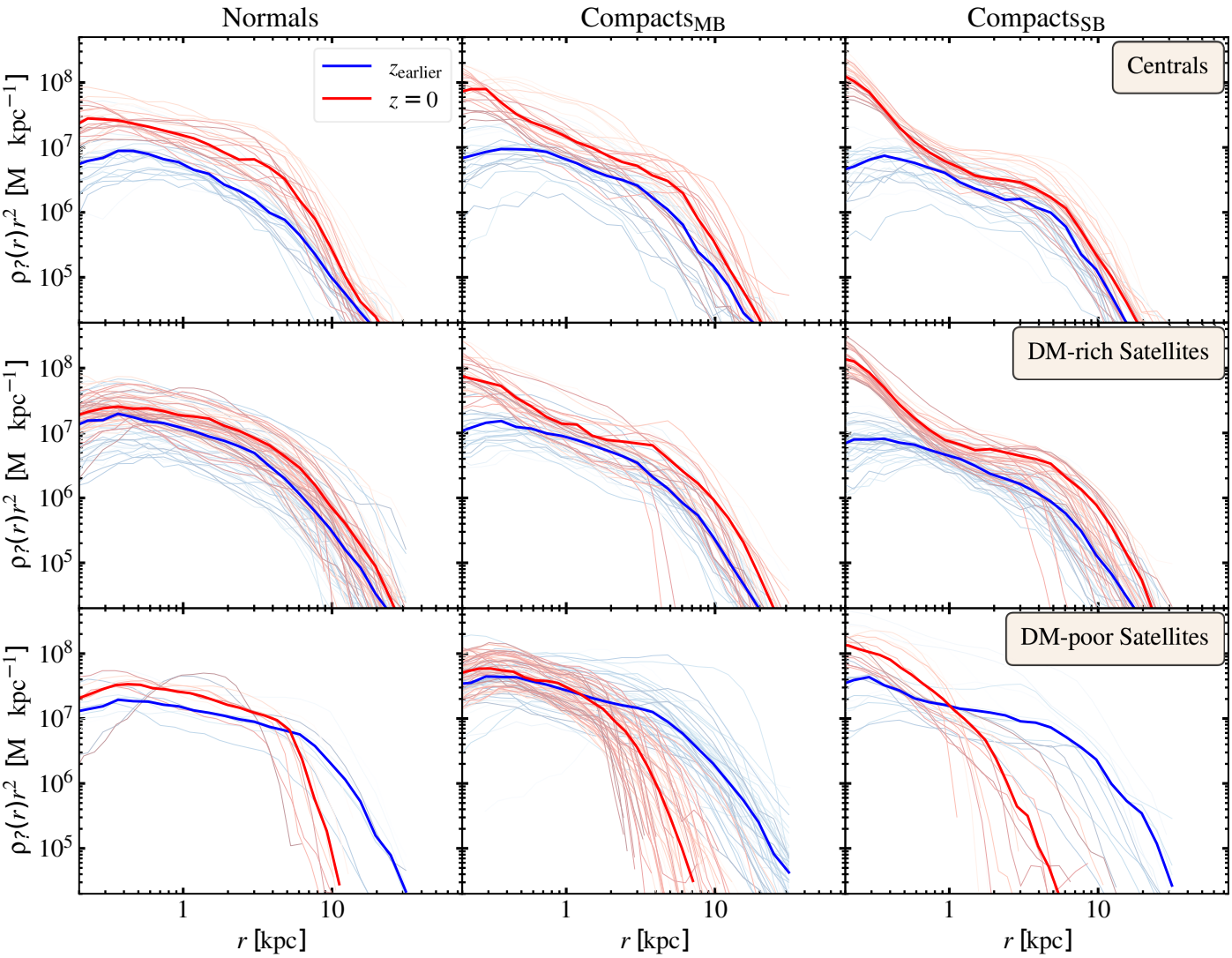

Figure 4. Stellar density profile at two different. The **left**, **middle** and **right** columns are for Normals, Compacts$_{MB}$, and Compacts$_{SB}$, respectively. The **first**, **second** and **third** lines are for Centrals, DM-rich Satellites, and DM-poor Satellites, respectively. The *blue* and *red lines* are for $z_{earlier}$ (which corresponds to 1 for centrals and DM-rich Satellites and to z_{entry} for DM-poor Satellites), and $z = 0$, respectively. The **bold lines** are for median radial profiles.

Acknowledgements. APA thanks the São Paulo Research Foundation, FAPESP, for financial support through contracts 2022/05059-2 and 2020/16152-8. G.B.L.N. thanks financial support from CNPq (grant 314528/2023-7) and FAPESP (grant 2024/06400-5).

References

Bekki, K., Couch, W. J., & Drinkwater, M. J. 2001, ApJL, 552, L105
Bekki, K. 2008, MNRAS, 388, L10
Brodie, J. P., Romanowsky, A. J., Strader, J., & Forbes, D. A. 2011, AJ, 142, 199
Chilingarian, I. V. & Mamon, G. A. 2008, MNRAS, 385, L83
De Almeida, A. P., Mamon, G. A., Dekel, A., & Lima Neto, G. B. 2024, A&A, 687, A131
De Almeida, A. P., Mamon, G. A., Dekel, A., & Lima Neto, G. B. 2024b, submitted
Dekel, A. & Silk, J. 1986, ApJ, 303, 39
Gunn, J. E. & Gott, J. Richard, III. 1972, ApJ, 176, 1
Haynes, Martha P., Dwarf Galaxies: From the Deep Universe to the Present, IAU Symposium, 2019, 344, 3-16
Marinacci, F., Vogelsberger, M., Pakmor, R., et al. 2018, MNRAS, 480, 5113
Merritt, D. 1983, ApJ, 264, 24
Mieske, S., Hilker, M., & Infante, L. 2002, A&A, 383, 823
Moore, B., Katz, N., Lake, G., Dressler, A., & Oemler, A. 1996, Nature, 379, 613
Naiman, J. P., Pillepich, A., Springel, V., et al. 2018, MNRAS, 477, 1206
Nelson, D., Pillepich, A., Springel, V., et al. 2018, MNRAS, 475, 624
Nelson, D., Pillepich, A., Springel, V., et al. 2019, MNRAS, 490, 3234
Pfeffer, J. & Baumgardt, H. 2013, MNRAS, 433, 1997
Pfeffer, J., Griffen, B. F., Baumgardt, H., & Hilker, M. 2014, MNRAS, 444, 3670
Pillepich, A., Springel, V., Nelson, D., et al. 2018, MNRAS, 473, 4077
Pillepich, A., Nelson, D., Springel, V., et al. 2019, MNRAS, 490, 3196
Silk, J. & Rees, M. J. 1998, A&A, 331,
Springel, V., Pakmor, R., Pillepich, A., et al. 2018, MNRAS, 475, 676